THE ASTROPHYSICAL JOURNAL, 443:786–794, 1995 April 20

THE SPECTRUM AND PULSES OF 1E 2259+586 FROM *ASCA* AND BBXRT OBSERVATIONS

R. H. D. CORBET[1]
Department of Astronomy and Astrophysics, 525 Davey Laboratory, Pennsylvania State University, University Park, PA 16802; corbet@astro.psu.edu
A. P. SMALE
Laboratory for High Energy Astrophysics, NASA/Goddard Space Flight Center, Greenbelt, MD 20771; alan@osiris.gsfc.nasa.gov
M. OZAKI AND K. KOYAMA
Department of Physics, Kyōto University, Sakyo-ku, Kyōto 606-01, Japan; ozaki@cr.scphys.kyoto-u.ac.jp, koyama@cr.scphys.kyoto-u.ac.jp
AND
K. IWASAWA
Department of Astrophysics, Nagoya University, Furo-cho, Chikusa-ku, Nagoya 464-01, Japan; iwasawa@phys.nagoya-u.ac.jp
Received 1994 September 8; accepted 1994 October 27

ABSTRACT

The 7 s X-ray pulsator 1E 2259+586 was observed for approximately 1 day in 1993 with *ASCA*. Observations were also obtained with BBXRT in 1990 a few months after *Ginga* had observed 1E 2259+586 to be brighter than normal and the BBXRT data show 1E 2259+586 to be at an intermediate brightness level. By contrast, the *ASCA* data appear to have been obtained during a more common lower luminosity state. The pulse profiles we obtain are consistent with a connection between flux and pulse shape reported from *Ginga* data, and the pulsator continues to spin down. We use our high spectral resolution data to search for cyclotron lines in the spectrum that were claimed from observations made with other satellites. We find that the *ASCA* spectra of 1E 2259+586 cannot be satisfactorily fitted with either a single power law or a combination of two power laws, and that significant residuals occur around 1.5 and 5 keV. However, a combination of a power law and a blackbody gives a good fit over the entire *ASCA* energy band with no evidence of spectral features. We have reanalyzed a *Ginga* LAC spectrum and find that this is also significantly better fitted by this two-component spectrum than a single power law. A possible explanation for such a two-component spectrum is that the blackbody emission comes from a neutron star and that the power-law component comes, at least in part, from a surrounding nebula.

As there has, so far, been no direct evidence that 1E 2259+586 is a binary system we consider whether there are other plausible mechanisms that might power the observed X-ray emission.

Subject headings: binaries: close — stars: individual (1E 2259+586) — stars: neutron — X-rays: stars

1. INTRODUCTION

1E 2259+586 is an X-ray pulsator with a period of approximately 7 s which has exhibited an approximately constant spin-down trend since its discovery. While 1E 2259+586 is thought to be a low-mass X-ray binary, there has, so far, been no direct evidence of this. An orbital period of 2300 s was reported by Fahlman & Gregory (1983) based on *Einstein* observations but this was not confirmed by more sensitive searches made with *Tenma* (Koyama, Hoshi, & Nagase 1987) and *EXOSAT* (Hanson et al. 1988; Morini et al. 1988). Observations with *Ginga* showed, at best, marginal evidence for an orbital period of 2120 s (Koyama et al. 1989).

The strongest evidence that 1E 2259+586 is an X-ray binary comes from the source luminosity of $\sim 2 \times 10^{35}$ ergs s^{-1} which is too great to be accounted for by the spin-down rate of $\sim 5 \times 10^{-13}$ s s^{-1}. Koyama et al. (1987) argued that the slow spin-down rate implies that 1E 2259+586 contains a neutron star rotating close to its equilibrium period and obtained a magnetic field of $\sim 5 \times 10^{11}$ G. Hanson et al. (1988) used the actual value of the spin-down rate to derive an equilibrium period for 1E 2259+586 of ~8.6 s and a magnetic field of $\sim 2.5 \times 10^{11}$ G. Apparent confirmation of a magnetic field in the range derived by these authors came when *Ginga* observations performed by Koyama et al. (1989) showed spectral structures around 5–10 keV which, if interpreted as cyclotron features, imply a magnetic field of $\sim 5 \times 10^{11}$ G. This spectral structure was also present in additional *Ginga* observations reported by Iwasawa, Koyama, & Halpern (1992, hereafter I92).

I92 reported that the spin-down rate of 1E 2259+586 had decreased compared to earlier observations. They suggested that this was connected with an increase in source luminosity and a change in pulse profile. A change in the spin-down rate would also be strong evidence that emission from 1E 2259+586 is powered by accretion, rather than spin-down of a neutron star. However, a single measurement of the pulse period cannot differentiate between a decrease in the spin-down rate and a model such as that considered by Usov (1994) which involves glitches in a rapidly rotating magnetic white dwarf.

1E 2259+586 lies in the supernova remnant G109.1−1.0 (Gregory & Fahlman 1980; Hughes, Harten, & van den Bergh 1981) suggesting a connection between the two. There is, however, no detectable large-scale radio or X-ray emission to the west of 1E 2259+586 which is probably connected with the presence of a giant molecular cloud in this region (e.g., Heydari-Malayeri, Kahane, & Lucas 1981; Tatematsu et al. 1985, 1987). G109.1−1.0 has an estimated age of 10^4 yr and a distance of 3.6–4.7 kpc. There has so far been no definite inden-

[1] Present address: Code 666, NASA/GSFC, Greenbelt, MD 20771.

tification of an optical companion, and Coe & Jones (1992) find that the optical identification of an optical companion, and Coe & Jones (1992) find that the optical counterpart cannot be brighter than a main-sequence K star. An apparent jetlike structure links 1E 2259+586 with G109.1−1.0 to the east, and there is a compact radio source to the west of 1E 2259+586 (Hughes et al. 1981).

In this paper we report on X-ray observations of 1E 2259+586 made with *ASCA* and BBXRT. The spectra obtained have considerably higher spectral resolution than in any of the previous studies. We search for the spectral features attributed to cyclotron lines by previous authors, and, in addition, update measurements of the pulse period and pulse profile.

2. OBSERVATIONS

2.1. *BBXRT*

The Broad Band X-Ray Telescope (BBXRT) was flown as part of the Astro-1 payload on the space shuttle Columbia in 1990 December. BBXRT consisted of two co-aligned telescopes, each equipped with solid-state detectors (Serlemitsos et al. 1992). Each detector was subdivided into five pixels with 512 energy channels; the central pixels (A0, B0) had a field of view 4.′5 in diameter, and the outer pixels (A1–A4, B1–B4) extended the total field of view to 17.′4. The B detectors were rotated relative to the A detectors such that, for example, A2 and B4 observed the same area on the sky. The detectors had an energy resolution of 9% at 1 keV and 2.5% at 6 keV and covered the energy range 0.3–12 keV with an on-axis effective area of ~ 150 cm^2 at 2 keV and ~ 80 cm^2 at 7 keV for each telescope/detector combination.

An observation of 1E 2259+586 was performed on 1990 December 5, with a total exposure time of 2240 s. These data were thus acquired approximately 4 months after the second *Ginga* observation presented by I92, in which 1E 2259+586 was found to be twice as bright as in other *Ginga* and *Tenma* observations.

The pulsar was observed 6.′2 off axis, such that the source flux fell mainly into the A2/B4 pixels. Figure 1 shows the fields of view of the BBXRT pixels projected onto an X-ray map of the G109.1−1.0 field derived from an *Einstein* IPC image.

2.2. *ASCA*

1E 2259+586 was observed for approximately 78,000 s on 1993 May 30–31 using the GIS and SIS detectors on board *ASCA*. The GIS and SIS detectors and the satellite itself are described in detail by Makishima et al. (1994), Ricker et al. (1994), and Tanaka, Inoue, & Holt (1994), respectively. Each of the four detectors (two GIS and two SIS) have collecting areas of approximately 250 cm^2. The GIS has an energy resolution of approximately 7.8% at 5.9 keV while that of the SIS is $\sim 2\%$ at the same energy.

The GIS detectors were operated in the PH mode which gives temporal resolutions of 0.0625 and 0.5 s in "high" and "medium" rate data collection modes, respectively, which are sufficient to provide phase resolved spectra of 1E 2259+586.

The SIS detectors were run in "Bright" and "Faint" modes utilizing all four CCDs in each detector, and thus the SIS data

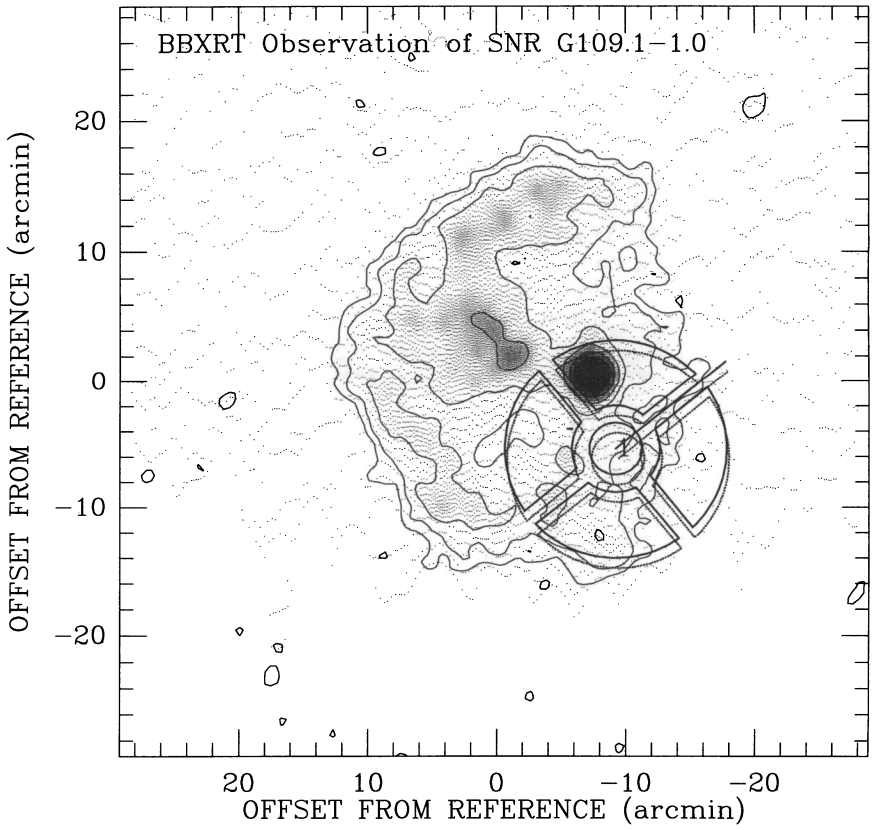

FIG. 1.—BBXRT pixel configurations projected onto a contour plot showing the X-ray surface brightness distribution of the G109.1−1.0 region, derived from an *Einstein* IPC image (sequence 9984). The image is centered at R.A. = $22^h59^m59^s.76$, decl. = +58°36′00″ (1950.0), and north is at the top of the figure. The contour levels represent 1, 2, 4, 8, 16, 32, and 64% of the peak flux in the image. The solid line shows the FOV and orientation of the pixels in the A-detector; the dotted line, the B pixels. The A1/A2 (B3/B4) border is also marked.

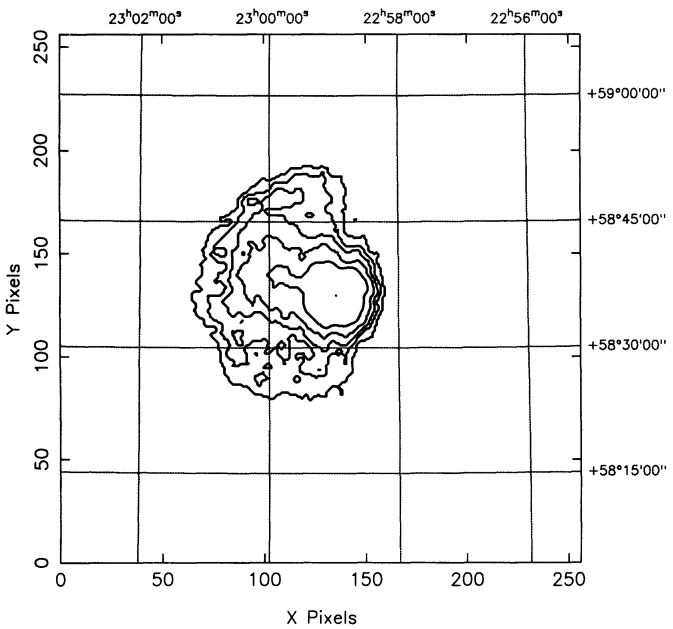

FIG. 2.—Image of the region containing G109.1 − 1.0 and 1E 2259 + 586 obtained with the *ASCA* GIS detectors.

do not have sufficient temporal resolution to provide phase-resolved spectra. However, these instruments do give significantly better spectral resolution and have somewhat better spatial resolution. The GIS provides a rather larger field of view than does the SIS and so covers a greater fraction of G109.1 − 1.0. The image of the region containing G109.1 − 1.0 and 1E 2259 + 586 obtained with the *ASCA* GIS detectors is presented in Figure 2.

3. RESULTS

3.1. *Pulse Timing*

Due to the short duration of the BBXRT observation the precision with which we can measure the pulse period is limited, and we obtain a value of 6.97895 ± 0.00053 s. For the *ASCA* GIS data we used a pulse arrival technique to obtain a pulse period of $6.9788465 \pm 5.6 \times 10^{-6}$ s. The pulse profiles obtained are shown in Figure 3 and the pulse period history of 1E 2259 + 586 is shown in Figure 4.

3.2. *Source Spectrum*

Figure 5 shows the spectrum of 1E 2259 + 586 derived from the BBXRT A2 and B4 pixels. Contamination from G109.1 − 1.0 is minimal; the SNR emission is both much softer and much weaker than that of the pulsar (see Rho & Petre 1994), and experimentation with various methods of subtracting SNR emission did not cause significant change to the spectral fitting results. A good fit to the pulsar spectrum is obtained with a simple power law plus absorption, with photon index $\Gamma = 3.86 \pm 0.10$ and column density $N_H = 1.01 \pm 0.06 \times 10^{22}$ cm^{-2}, and a χ^2 of 456/399 = 1.14. After compensating for a small amount of residual contamination from the bright Earth at 0.8 keV, the final χ^2 becomes 372/396 = 0.94. We also accumulated phase-resolved spectra and fit these individually. However, we found no statistically significant differences from the phase-averaged spectrum.

We also attempted to fit a simple absorbed power-law model to the *ASCA* GIS and SIS data on 1E 2259 + 586. For these fits we used only the energy range above 0.7 keV because of possible uncertain instrumental calibration at lower energies. The spectra were rebinned so as to ensure at least 20 photons in each bin. Due to the sharply falling source spectrum with energy this effectively reduces our spectral resolution at higher energies.

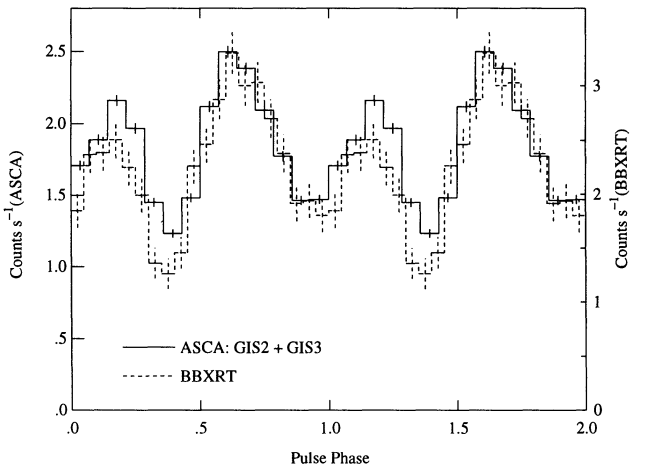

FIG. 3.—Pulse profile of 1E 2259 + 586 as observed with (1) the GIS detectors on board *ASCA* and (2) BBXRT. The pulse profiles from the two satellites are plotted with equal pulse maxima. Corrections for background levels have been made.

The *ASCA* mirrors appear to cause a small emission feature at ~2 keV for both the GIS and SIS detectors. The GIS response matrices available at the time of analysis contain a correction for this feature, while those for the SIS do not. For this reason, for all SIS spectral fits we also included an emission line with central energy and width fixed at the presently

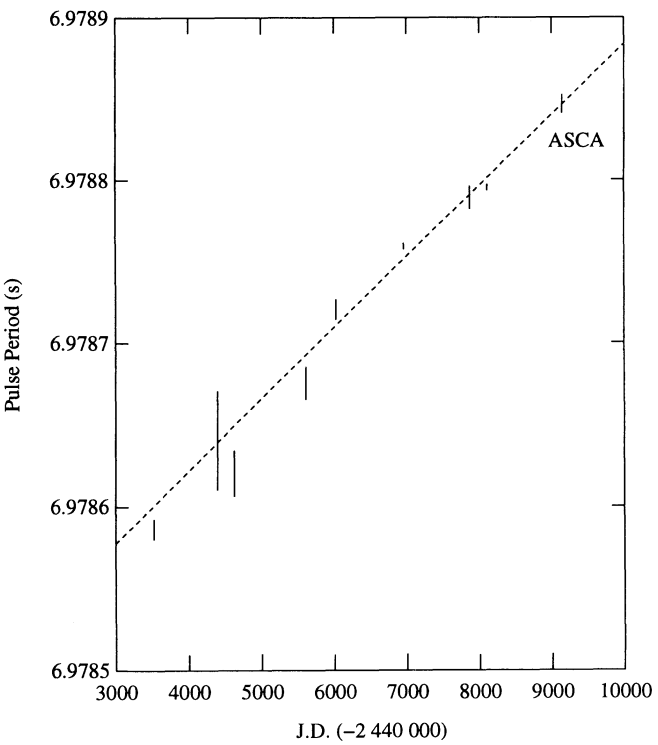

FIG. 4.—Spin period history of 1E 2259 + 586. The dashed line is the best-fit straight line to all the values. The pulse period derived from the BBXRT data is not shown due to the large error on this value.

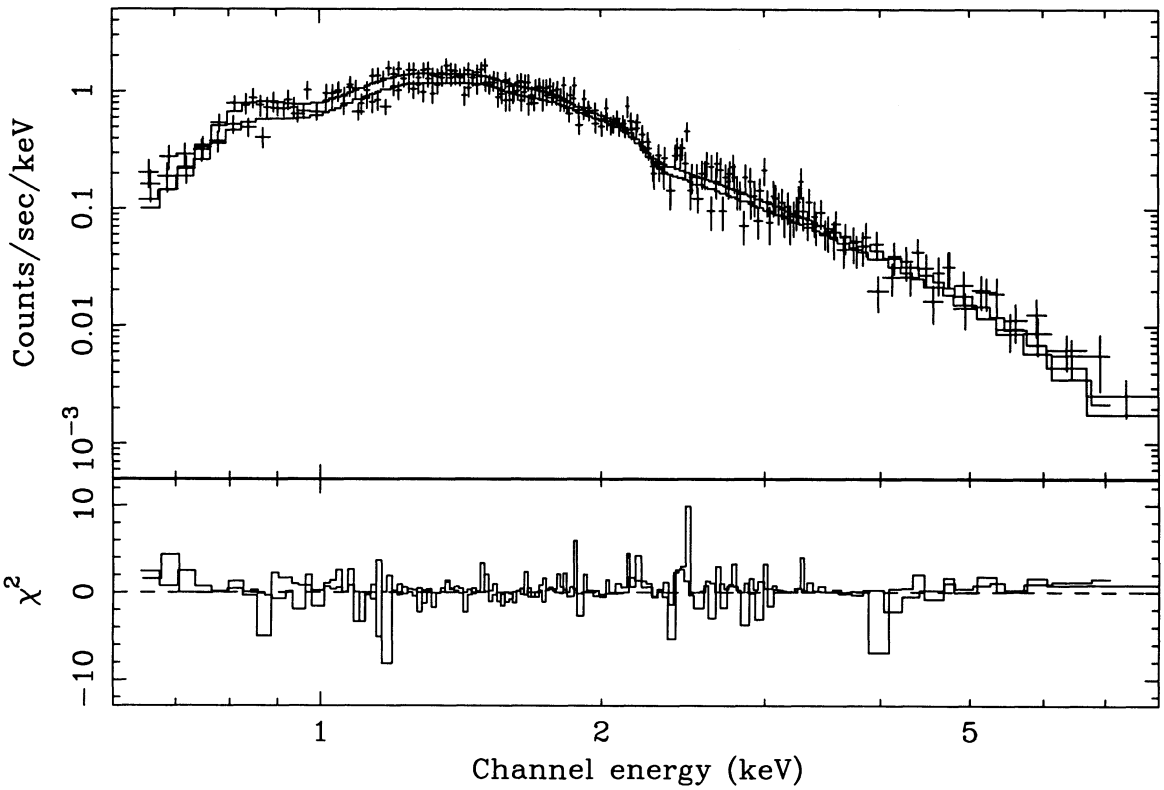

FIG. 5.—The spectrum and best-fit power law to the BBXRT data. A simultaneous fit was performed on the A2 and B4 pixels. The spectra have been rebinned to improve the signal-to-noise ratio. Spectral parameters are given in Table 1.

best determined values of 2.2 keV and 100 eV, respectively, and only the line normalization was allowed to vary.

For all four detectors we found that in no case could a good fit be obtained with a simple power law (see Fig. 6*a* and Table 1). In addition, the major residuals from the fitted model all occur in the 1–2 keV region and around 5 keV. We also attempted to use the two-component power-law model adopted by I92 and found that this gave essentially the same results as a single power law. We next attempted to model the residuals in terms of absorption lines or edges. While this worked reasonably well for the ~1 keV residuals, any attempt to fit a feature at ~5 keV resulted in this feature migrating to lower energies, becoming very broad and hence modifying a large fraction of the continuum. We therefore experimented with using other continuum models. The "standard" X-ray pulsar model of a power law with a high energy cutoff gave a moderately good fit. However, the "high-energy" cutoff starts at an unrealistically low value of ~2 keV and still gave significant residuals at >5 keV. We eventually determined that a good fit across our energy band could be obtained using a combination of a power law together with a blackbody (Fig. 6*b*). While a power law plus thermal bremsstrahlung gave only a slightly worse fit, the slope of the power-law component (~0), does not have a simple interpretation as does the power-law component derived from the blackbody/power-law fit (see § 4).

TABLE 1

RESULTS OF SPECTRAL FITS TO 1E 2259+586

Instrument	χ^2	N_H ($\times 10^{22}$ cm^{-2})	Γ	$kT_{blackbody}$ (keV)
S0	2.36	1.25	3.99	...
	0.93	0.67 ± 0.09	3.04 ± 0.31	0.415 ± 0.007
S1	2.39	1.25	4.04	...
	1.42	0.76 ± 0.13	3.32 ± 0.37	0.409 ± 0.009
G2	1.53	1.15	4.17	...
	1.02	0.43 ± 0.11	3.15 ± 0.26	0.418 ± 0.007
G3	1.67	1.23	4.24	...
	1.01	0.48 ± 0.10	3.29 ± 0.23	0.423 ± 0.006
BBXRT	1.14	1.01	3.86	...
	0.92	0.88 ± 0.11	3.34 ± 0.24	0.329 ± 0.017
Ginga (2–20 keV)	29.7	0.00	3.59	...
	4.5	0.00	2.28	0.37

NOTE.—All errors are 1 σ single-parameter confidence levels.

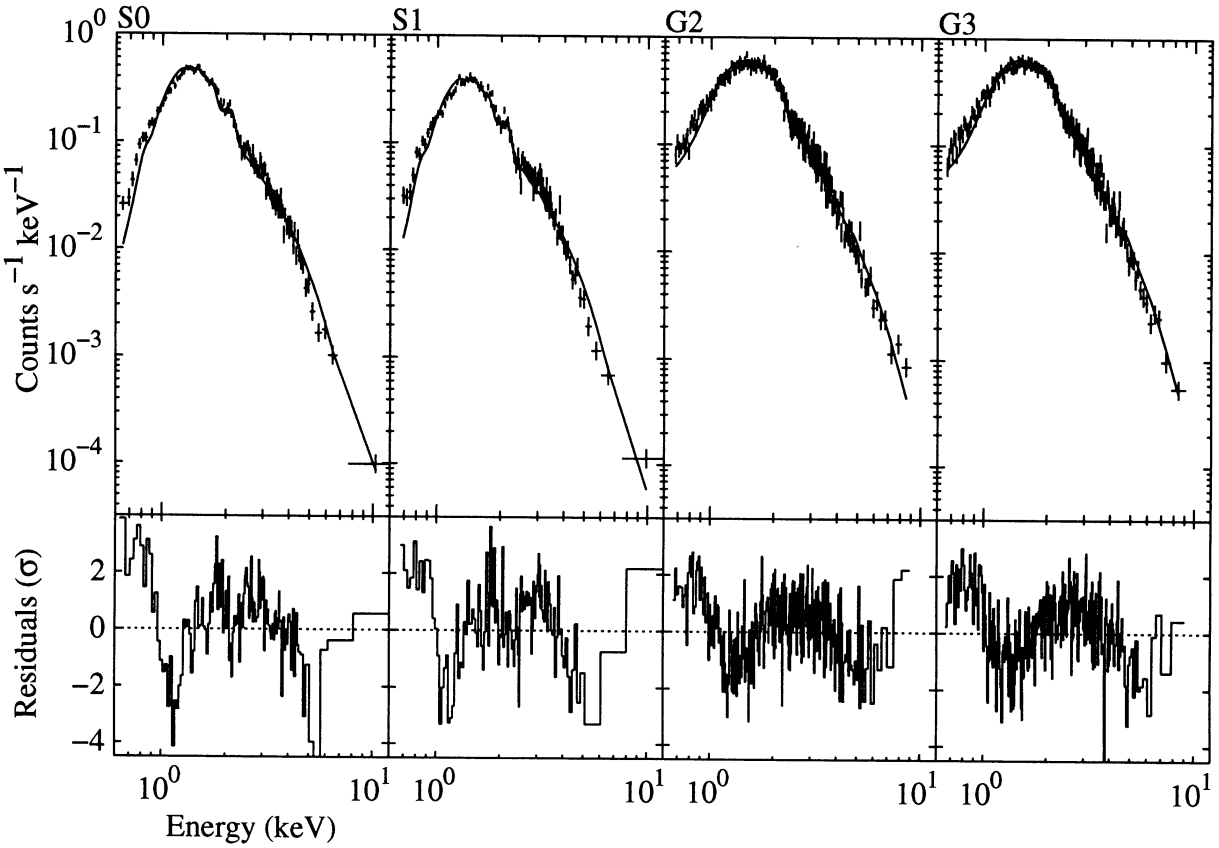

FIG. 6*a*

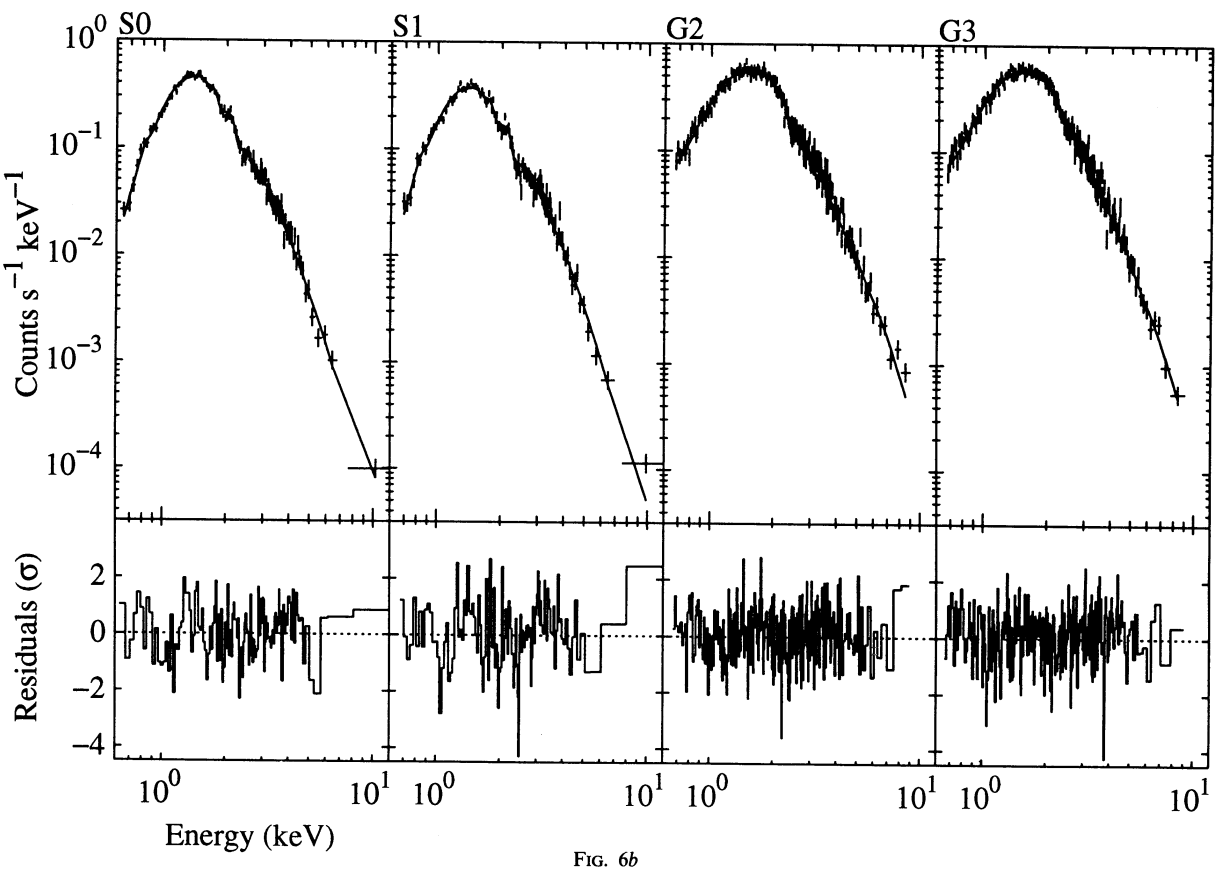

FIG. 6*b*

FIG. 6.—(*a*) Fits to the *ASCA* spectra from all four detectors using a simple absorbed power law. Parameters are given in Table 1. (*b*) Fits to the *ASCA* data from all four detectors using a combination of a power law and a blackbody spectrum. Parameters are given in Table 1.

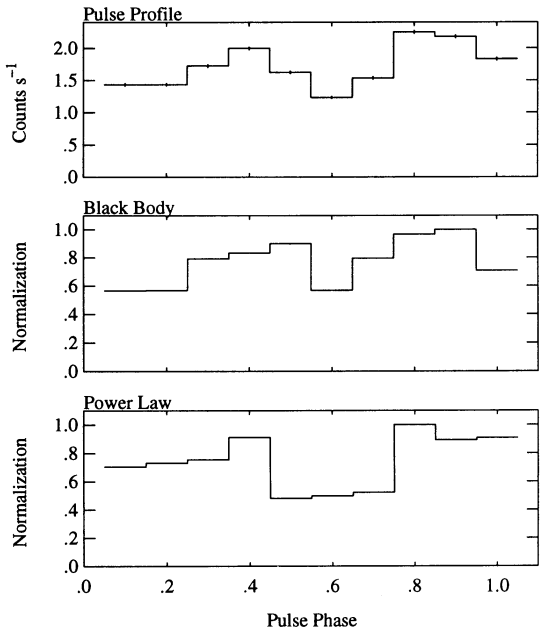

FIG. 7.—Contributions of the two spectral components to pulse phase resolved spectra of 1E 2259+586 obtained with the *ASCA* GIS detectors.

As a simple power law does not fit the *ASCA* spectra well we reexamined the BBXRT spectra and fitted a power law plus blackbody. This also gave an improved fit with no systematic residuals at any energies, and the best fit parameters are similar to those derived from the *ASCA* spectra (Table 1).

The GIS data were divided into 10 phase bins, and these were fitted individually using the same power-law plus blackbody model. Although the normalization of the blackbody component bears a stronger resemblance to the pulse profile (Fig. 7) the normalization of the power-law component indicates that either this component is also pulsed or that our fitting procedure fails to adequately separate these two spectral components. In order to search for phase-dependent features, we also constructed plots of the ratio of phase-resolved spectra to the summed spectrum. This procedure failed to show the presence of phase-dependent features.

3.3. *Reanalysis of Ginga Spectra*

We have taken the LAC spectrum from the 1989 *Ginga* (I92) observation and also attempted to fit it with a power-law plus blackbody model. We find that this model gives a considerably better fit to the data than does a single power law (Table 1). However, the fit is still formally unacceptable with the residuals from the fit displaying some amount of structure (Fig. 8). The spectral parameters, including the slope of the power law, are also somewhat different from those found from the *ASCA* and BBXRT spectra.

4. DISCUSSION

4.1. *Spectra*

X-ray emission comes a number of sites in the vicinity of 1E 2259+586: the SNR G109.1−1.0, the "jet," and 1E 2259+586 itself. With *ASCA* we are able to obtain spectra of each of these components separately, and, although limited spatial deconvolution was possible in the observations of Morini et al. (1988), this was not the case for most previous observations of 1E 2259+586. In particular, the observations by Koyama et al. (1987) and I92 in which cyclotron lines were reported were made with the *Ginga* LAC which was collimated proportional counter with a field of view of approximately 1° × 2°. It is reassuring that we find, for example, that the spectrum of the

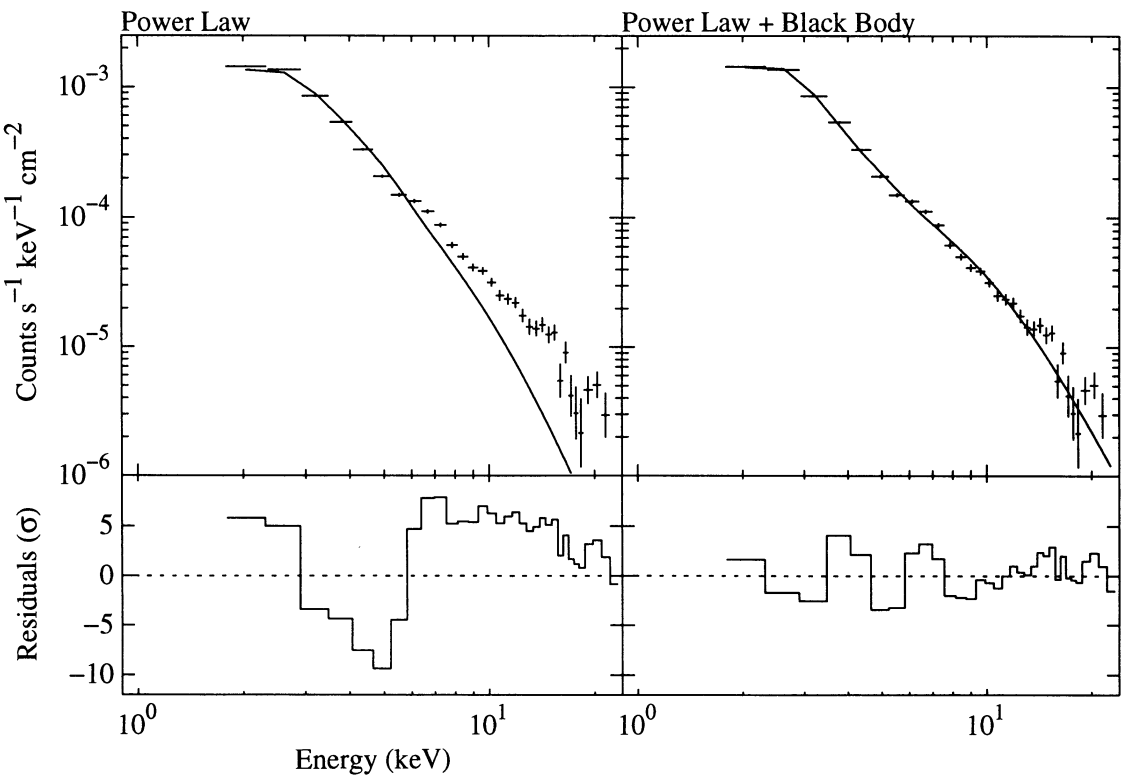

FIG. 8.—The spectrum of 1E 2259+586 obtained in 1989 with the *Ginga* LAC detector and the best-fit power law (*left*) and power law plus blackbody (*right*)

"jet" has very little flux at higher energies where line features in the spectrum of 1E 2259+586 have been reported (Fig. 9). However, there has also been a recent report of extended emission (perhaps a synchrotron nebula) around 1E 2259+586 by Rho & Petre (1995) from *ROSAT* PSPC observations which can be fitted with a power-law spectrum with $\Gamma \sim 3.4$. Due to the larger point-spread function of *ASCA* compared to *ROSAT*, such a nebula cannot easily be detected in our data. We note that the spectral index of the power-law component in our fits to the spectra of 1E 2259+586 is very similar to that of the nebula. For the blackbody component, the derived radius is ~3 km for a distance of 4 kpc which would be consistent with emission from a neutron star surface. The *ASCA* fits indicate that approximately 58% of the unobscured luminosity in the 1–10 keV range comes from this blackbody component. This indicates that both components are too luminous to be accounted for by the spin-down luminosity of a neutron star.

The presence of features in the *Ginga* spectra was derived using a continuum model which was a sum of two power laws. The fits to our *ASCA* data show that this type of model can lead to apparently spurious features. The *Ginga* spectral results should therefore be treated with caution. Although features are still apparent in the *Ginga* spectra when we fitted the power-law plus blackbody model, the presence of a number of contributing sources to the *Ginga* spectra, together with an uncertain background subtraction at higher energies (e.g., I92), make it difficult to show unequivocally that these features are really coming from 1E 2259+586 itself.

4.2. *Pulses*

The *Ginga* observation that was made in 1990 showed 1E 2259+586 to be about a factor of 2 brighter at a level of 1.0×10^{35} ergs s^{-1} $(d/4 \text{ kpc})^2$ (2–10 keV) than during other observations that were made with *Ginga* and *Tenma* (I92). It was also found that the pulse profile had changed and the two peaks in the pulse profile had become more unequal. The BBXRT observations were made a few months after this *Ginga* observation and imply a luminosity of 0.8×10^{35} ergs s^{-1}. The pulse profile in the BBXRT observations appears to be somewhat intermediate between the 1990 *Ginga* profile and the "quiescent" profile. In contrast, the *ASCA* observations show a flux and a pulse profile which are comparable to the quiescent state.

From Figure 2 of I92 we estimate main peak to secondary peak ratios of approximately 1.4 for the brighter observation and 1.13 for the fainter observation. For the BBXRT observation the ratio is ~1.3 and for the *ASCA* GIS data the ratio is ~1.14. This difference between the BBXRT and *ASCA* pulse profiles can clearly be seen in Figure 3. The *ASCA* spectra imply a 2–10 keV luminosity of approximately 0.33×10^{35} ergs s^{-1} which is consistent with the "quiescent" *Ginga* luminosity. The pulse profiles measured with *EXOSAT* also show a peak ratio of ~1.14 in the range 1.2–5.2 keV (Hanson et al. 1988) while the *Tenma* pulse profiles are rather too noisy to give a precise measurement of the pulse-peak ratio.

The pulse profiles obtained with *Einstein* by Fahlman & Gregory (1983) also show changes in shape. However, these appear to show the opposite behavior from results with other missions. The pulse profiles obtained in 1980 July at a count rate of 0.9 s^{-1} show approximately equal peaks unlike the more asymmetric profiles measured in 1981 January at a lower count rate of ~0.8 s^{-1}. However, the *Einstein* IPC energy response is considerably softer than that of *ASCA*, *Ginga*, and *Tenma*. *ASCA* and BBXRT, however, have similar energy responses which are slightly softer than those of *Ginga* and *Tenma*.

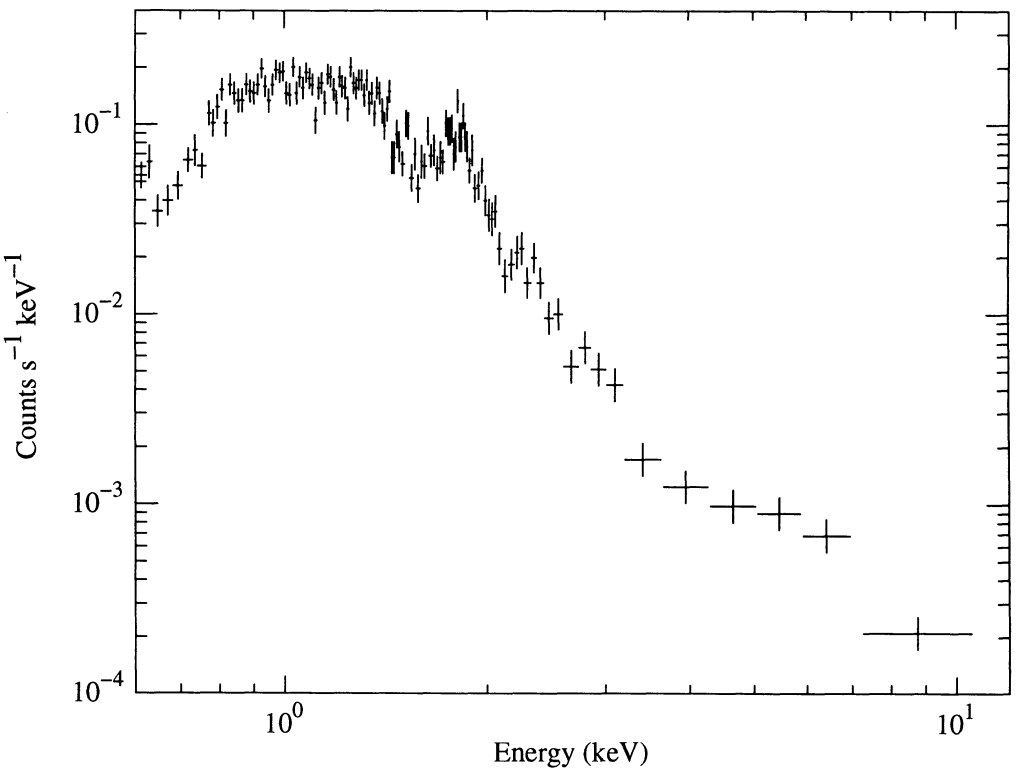

FIG. 9.—Spectrum of the "jet" obtained with GIS 2

The pulse period that we obtain from the *ASCA* observations does not confirm the decrease in spindown rate reported by I92, and either a change in spindown rate or glitches, such as favored by Usov (1994) can, in principle, explain our results. However, the return to the previous spindown rate is consistent with the source returning to the previous luminosity level.

4.3. *Is 1E 2259+586 Really a Binary?*

Although the hypothesis that 1E 2259+586 is a binary system has been strongly favored, we have yet to find any direct evidence for binarity—there is no detectable Doppler modulation of the X-ray pulses, and no optical counterpart has been identified. While a model involving a spinning-down white dwarf has been proposed by Morini et al. (1988) and Paczyński (1990), this would not be consistent with the spectral features reported by I92 if these are interpreted as cyclotron lines. We therefore now consider whether other alternatives to the binary model are plausible.

4.3.1. *Accretion from the Molecular Cloud*

We note that 1E 2259+586 is located right at the edge of G109.1−1.0 where the supernova shock wave is believed to be impinging on a molecular cloud. To determine whether accretion from the surrounding medium can power the observed X-ray luminosity, we need to estimate the density and relative velocity of the medium. We assume that the neutron star is outside the shell of the supernova remnant. A very crude estimate of the transverse velocity of the neutron star comes from the separation of 1E 2259+586 from the center of G109.1−1.0 and the estimated age of G109.1−1.0. This gives a velocity of ~ 600 km s^{-1}; for comparison Rho & Petre (1994) estimate a velocity of 760 km s^{-1} for the shell of G109.1−1.0. Rho & Petre also estimate a density of 1.2 cm^{-3} for the X-ray–emitting shell of the supernova remnant. In order for the neutron star to be accreting from the molecular cloud, it is necessary for the velocity of the neutron star to be greater than that of the shell, at least where the shell impinges on the cloud, so that the neutron star may overtake the shell.

If we assume that Bondi-Hoyle–type accretion takes place and that all material passing within the capture radius (determined by setting kinetic energy equal to potential energy) is accreted, then, in order to account for the observed luminosity, we require a density

$$D \sim 10^6 v_{100}^3 L_{35} \text{ H cm}^{-3} ,$$

where v_{100} is the relative velocity in units of 100 km s^{-1} and L_{35} is the luminosity in units of 10^{35} ergs s^{-1}. If we assume that the neutron star is rotating near its equilibrium period with Alfvén radius equal to the corotation radius (cf. Corbet 1984) we obtain:

$$D \sim 10^6 v_{100}^3 B_{5e11}^2 \text{ H cm}^{-3} ,$$

where B_{5e11} is the magnetic field of the neutron star in units of 5×10^{11} G.

As noted by I92, the luminosity measured with *Ginga* and the magnetic field strength inferred from the spectrum are consistent with equilibrium rotation.

For comparison, Tatematsu et al. (1987) discuss densities of 200 H cm^{-3} in the molecular cloud. If the molecular cloud is compressed by the supernova remnant, we might expect even higher local densities. In addition, if the cloud is swept up by the supernova shell, this may also reduce the relative velocity between the neutron star and the surrounding medium somewhat.

This relatively low velocity and moderate density would be somewhat reminiscent of accretion from the envelope of a Be star circumstellar envelope. In the case of accretion from a Be star envelope, it is possible that an accretion disk may form. For accretion from the surrounding medium, is there any way that a disk could form? This may be required from the rather steady spin down that is observed. The major difficulties with this model are

1. Is the neutron star actually inside the molecular cloud?
2. Is the density of the cloud sufficient to account for the observed X-ray luminosity? Unless the molecular cloud is exceptionally dense in the region of the neutron star a relative velocity of ~ 5 km s^{-1} is indicated.
3. Is the lack of angular momentum in the accreted matter a problem? Neutron stars which accrete from stellar winds (which have low angular momentum) display erratic spin up and spin down behavior instead of the rather constant spin-down trend exhibited by 1E 2259+586 (cf. Nagase 1989).

4.3.2. *Accretion from Circumstellar Debris?*

While accretion from the molecular cloud might be plausible, are there any other sources of matter that could power the observed X-rays? One possibility is to extend the speculative model put forward by Katz, Toole, & Unruh (1994) to explain soft gamma-ray repeaters (SGR). These authors explore a model where a supernova leaves planets orbiting a neutron star in intersecting orbits. These planets then collide to produce debris, some fragments of which fall onto the neutron star to produce gamma-ray bursts. We now consider whether such circumstellar debris might also be able to power X-ray emission. The mean luminosity of $\sim 10^{35}$ ergs s^{-1} implies a mass accretion rate of $\sim 10^{15}$ g s^{-1}. If the age of 1E 2259+586 is the same as that of G109.1−1.0 at $\sim 10^4$ yr, then a lifetime accretion of $\sim 10^{-7}\ M_\odot \simeq 0.06\ M_{\text{Earth}}$ is implied. Accretion from a circumstellar envelope would naturally have angular momentum—avoiding the possible problems with the molecular cloud accretion model above. If we make the simplifying assumption that 1E 2259+586 contains a neutron star rotating at its equilibrium period, P, which depends on the accretion rate, and that the accretion rate in turn depends on the mass of the circumstellar envelope, M, such that $P \propto M^{-n}$, then

$$M = -n\dot{M}(P/\dot{P}) .$$

For a luminosity of 10^{35} ergs s^{-1} and an accretion efficiency of 10% (i.e., $L_X = 0.1\ \dot{M}c^2$) we obtain a total circumstellar mass $\sim 2.5n\ M_{\text{Earth}}$. For comparison, Katz et al. (1994) consider collisions between planets of mass $3\ M_{\text{Earth}}$, which is the minimum mass of the planets around PSR B1257+12 (Wolszczan 1994).

Hence, on total system mass, spindown rate, and luminosity, the circumstellar mass requirements are not excessive—it does not require much mass to power a short-lived, low-luminosity X-ray source. Where our model differs from that of Katz et al. (1994) is that they consider "lumpy" accretion, which results in gamma-ray bursts, whereas we require a relatively constant accretion rate from both the long-term and short-term light curve. In fact Katz et al. do state that tidal disruption of accreting material could result in smaller fragments and perhaps fluid which could then accrete through a disk resulting in a low-luminosity X-ray source. It is, however, unclear whether dynamically a relatively constant accretion rate over a long period can be maintained from debris. The interpretation of the spin down rate as caused by a slow decrease in the mass of a circumstellar "envelope" also predicts that the source luminosity should be gradually decreasing. This is difficult to test

TABLE 2

COMPARISON OF 1E 2259+586 AND THE POINT SOURCE IN N49

Parameter	1E 2259+586	SGR 0525−66
Pulse Period (s)	6.98	8.0?
L_X (ergs s^{-1})	2×10^{35}	~ 7–9×10^{35}
Age of SNR (yr)	10^4	5.4×10^3
Location	Edge of SNR	Edge of SNR
"Jet"?.....	Yes	Possible
Optical Counterpart.....	None	None

observationally as measuring the mean source luminosity is much more difficult than accurately measuring the pulse period.

4.3.3. *Magnetars*

Thompson & Duncan (1993 and references therein) have proposed a model for SGRs which involves neutron stars with extremely strong magnetic fields which they term "magnetars." They have also applied this model to 1E 2259+586 and derive a magnetic field of $\sim 0.7 \times 10^{14}$ G. Their interpretation is that X-ray emission from 1E 2259+586 is powered by magnetic energy rather than accretion or spindown. The very high magnetic field strength required in this model is apparently excluded by the cyclotron features detected by I92. However, our discovery that, at least in the *ASCA* data, apparently spurious features can be produced depending on the continuum model employed, shows that an extremely large magnetic field strength may still be possible. The magnetar model also predicts that a blackbody spectrum with a temperature of a few tenths of a keV should be produced together with a nonthermal component (C. Thompson & R. C. Duncan, private communication). A key observational test of the magnetar model is that glitches should occur rather than changes in the spin-down rate.

4.3.4. *Is 1E 2259+586/G109.1−1.0 Similar to SGR 0525−66/N49?*

Extending our comparisons to SGRs we note that there are a number of apparent similarities (see Table 2) between G109.1−1.0 and the supernova remnant N49 which contains SGR 0525−66 and has an X-ray point source (Rothschild et al. 1994). Based on this similarity we have searched the BATSE catalog for bursts that would be consistent with the location of 1E 2259+586. While we find three bursts that are consistent with this position, there is no evidence for a statistically significant excess of bursts at this location compared to what would be expected by chance.

Whether these similarities are more than just coincidental can probably best be determined by better determining the properties (pulse period, spin down rate, and source spectrum) of the pointlike X-ray source in N49. We note that a number of the similarities between 1E 2259+586 and SGR 0525−66 were also independently commented on by Thompson & Duncan (1992).

5. CONCLUSION

Our *ASCA* spectra can be well fitted with a blackbody and power-law spectrum. An interpretation is that the blackbody emission is coming from 1E 2259+586 itself and that at least a portion of the power-law component comes from an extended nebula detected in *ROSAT* observations. However, the spectra from the nonimaging LAC on *Ginga* are not perfectly fit by this model. The ideal investigation of the spectrum of 1E 2259+586 would come from an observation which has sufficient spatial resolution to resolve 1E 2259+586 from the surrounding nebula together with good spectral resolution over a broad energy band.

Repeated continued monitoring of the pulsation period of 1E 2259+586 is required in order to differentiate between changes in spindown rate and glitches in the pulsation period. Extended pulse period monitoring would also provide additional information on the correlations between spindown rate, source luminosity, and pulse shape that are believed to exist

We thank R. Petre and J.-H. Rho for useful comments and providing details of their *ROSAT* observation; C. Thompson and R. Duncan for communicating details of their models; and NASA for partial support through grant NAG 5-2483.

REFERENCES

Coe, M. J., & Jones, L. R. 1992, MNRAS, 259, 191
Corbet, R. H. D. 1984, A&A, 141, 91
Fahlman, G. G., & Gregory, P. C. 1983, in IAU Symp. 101, Supernova Remnants and Their X-Ray Emission, ed. J. Danziger & P. Gorenstein (Dordrecht: Reidel), 445
Gregory, P. C., & Fahlman, G. G. 1980, Nature, 287, 805
Hanson, C. G., Dennerl, K., Coe, M. J., & Davies, S. R. 1988, A&A, 195, 114
Heydari-Malayeri, M., Kahane, C., & Lucas, R. 1981, Nature 293, 549
Hughes, V. A., Harten, R. H., & van den Bergh, S. 1981, ApJ, 246, L127
Iwasawa, K., Koyama, K., & Halpern, J. 1992, PASJ, 44, 9 (I92)
Katz, J. I., Toole, H. A., & Unruh, S. H. 1994, ApJ, 437, 727
Koyama, K., Hoshi, R., & Nagase, F. 1987, PASJ, 39, 801
Koyama, K., et al. 1989, PASJ, 41, 461
Makishima, K., et al. 1994, PASJ, in press
Morini, M., Robba, N. R., Smith, A., & van der Klis, M., 1988, ApJ, 333, 777
Nagase, F. 1989, PASJ, 41, 1
Paczyński, B. 1990, ApJ, 365, L9
Ricker, G. R., et al. 1994, PASJ, in press
Rho, J.-H., & Petre, R. 1994, in The Soft X-Ray Cosmos: *ROSAT* Science Symposium, ed. E. M. Schlegel & R. Petre (New York: AIP), 320
———. 1995, in preparation
Rothschild, R. E., Kulkarni, S. R., & Lingenfelter, R. E. 1994, Nature, 368, 432
Serlemitsos, P. J., et al. 1992, in Proc. of the 28th Yamada Conference of the Frontiers of X-Ray Astronomy, ed. Y. Tanaka & K. Koyama (Tokyo: Universal Academy), 221
Tanaka, Y., Inoue, I., & Holt, S. S. 1994, PASJ, 46, L37
Tatematsu, K., Fukui, Y., Nakano, M., Kogure, T., Ogawa, H., & Kawabata, K. 1987, A&A, 184, 279
Tatematsu, K., Nakano, M., Yoshida, S., Wiramihardja, S. D., & Kogure, T. 1985, PASJ, 37, 345
Thompson, C., & Duncan, R. C. 1992, in Compton Gamma-Ray Observatory, ed. M. Friedlander et al. (New York: AIP), 1085
———. 1993, ApJ, 408, 194
Usov, V. V. 1994, ApJ, 427, 984
Wolszczan, A. 1994, Science, 264, 538